Shear Strength between Cemented Paste Backfill

Jean-Frédéric N. Koupouli [a], T. Belem [a], P. Rivard [b]

[a]Research Institute in Mining and Environment, Université du Québec en Abitibi-Témiscamingue, Rouyn-Noranda, Canada
[b]Département de génie civil, Université de Sherbrooke, Sherbrooke, Canada

* Corresponding author. Patrice.Rivard@usherbrooke.ca.

Abstract. After placement underground, the physical–chemical and mechanical properties of unsaturated cemented paste backfill (CPB) will evolve over time due to self-weight consolidation and binder hydration. However, the behavior of the interface CPB-rock wall is not well known. This paper attempt to bring experimental results in order to better understand this behavior. The rock interface replicas were made from natural rock surfaces (schist and granite). Both frictional shear and shear bond strengths were determined. The results show that the shear strength at the schist interface (rougher) is higher than the one at the granite interface. The cohesion and the interfacial friction angle depend on the CPB curing time (hydration) and the applied normal stress.

Keywords. Cemented paste backfill, Rock surface, Shear strength, Cohesion, Friction angle

INTRODUCTION

Cemented paste backfill (CPB) technology is increasingly and widely used in many underground mines throughout the planet and has become popular over the last two decades (Potvin et al., 2005; Belem and Benzaazoua, 2008). CPB is obtained from mixing tailings with water and a binder. This technology was implemented in the Canadian mines in the early 90's (Landriault and Tenbergen, 1995). The technology implies the reuse of at least 50% of the full stream tailings as CPB for underground mine stopes filling. The role of the CPB is to serve as secondary ground support (Mitchell, 1989 ; Belem et al., 2000). Consequently, CPB can provide a stable working platform for miners, and it reduces the amount of open space that could potentially be filled with a collapse of the surrounding pillars. In order to retain the CPB during open stope filling, the structural barricades are designed to prevent any failure induced by high pressures generated by the fill mass. The proper design of a barricade requires a correct estimate of barricade loads, which in turn depend on the stress distribution within the backfilled stope (Belem et al., 2013).

In many cases, the adjacent rock sidewalls help supporting the fill through the interface shear strength and the arching phenomenon. Therefore, CPB and rock sidewalls may be mutually supporting (Mitchell, 1989). When arching occurs in a filled stope, the vertical stress at the bottom of the fill mass is lower than the overburden pressure due to horizontal stress transfer. This pressure transfer is primarily associated with the frictional and/or cohesive interaction between CPB and the rock sidewall (Belem and Benzaazoua, 2008). In situ measurements conducted by Le Roux et al. (2005) show that the pore-water pressure on barricades is negligible after a few days. If the CPB permeability is very low and water does not drain out under gravity, no settlement of the CPB occurs (Belem et al., 2013). However, without any settlement, no shear stress can be mobilized at the CPB–rock sidewall interface and no arching could occur. On the other hand, if the CPB desaturates to enable negative pore pressures generation it will in turn mobilize shear stresses at the fill–rock sidewall interface (Le Roux et al., 2005). The shear strength mobilized at the interface will depend on the level of friction, which is a function of the horizontal effective stress acting on the interface (Fourie et al., 2007). The determination of the shear stress development will allow understanding of how the arching effect can occur (and thus stress relief on barricades). This effect can be taken into account during the preliminary backfill design process (De Souza et al., 2009). It is therefore necessary to investigate the shear strength parameters experimentally and the shear stiffness of CPB–rock sidewall interfaces.

Very few experimental studies have been conducted on CPB–natural rock sidewall interface behavior. One study was carried out on the shear behavior of simulated backfill (SBkf)–limestone smooth interface (Nasir and Fall, 2008), followed by another made on SBkf–concrete and brick interfaces (Fall and Nasir, 2010). It was concluded that, for the same stress conditions, the shear strength of the SBkf materials was greater than that of the SBkf–limestone/concrete/brick interfaces. It was also suggested that the interfacial friction angle (δ) of SBkf–composite interfaces was greater than 2/3 of the internal friction angle (φ) of SBkf material ($\delta > 2/3\ \varphi$). For the design of a backfilled stope with an exposed free face, Mitchell et al., (1982) made the assumptions that (i) the backfill–rock sidewall interfacial cohesion (c_b) is equal to the cohesive strength of the backfill material (c), and (ii) $\delta = \varphi = 0$. Manaras (2009) performed direct shear tests on different CPB–concrete interfaces at various normal stress levels (35 to 1500 kPa) and three different curing times (14, 28 and 56 days). It was concluded that δ and the cohesion c_b increased with the amount of binder, the wall roughness, and the curing time.

The main objective of this paper is to conduct a laboratory investigation aiming at characterizing the shear stress–tangential displacement behavior and the determination of shear strength parameters of early age CPB.

MATERIALS

The tailings sample was taken from Casa Berardi mine (Hecla Mining Company, Quebec, Canada). After transferring to the lab, tailings barrels were homogenized. The binder used for backfill mixture is a blend of 20% general use Portland cement (GU) and 80% ground granulated blast furnace slag (GBFS). The binder content Bw% (= 100*Mbinder/Mdry-tailings) was 5% by dry mass of tailings.

Room-temperature-vulcanization (RTV) silicone was used for reproducing the natural rock surfaces accurately. Silicone is first poured over the targeted surface portions using a squared frame and left to harden. Artificial rock surface mortar replicas were prepared by pouring a blend of SikaGrout®212 and water (water-to-Sika ratio of 0.18, room temperature of approximately 23°± 2° C, and relative humidity ≥ 50%) over the previously obtained silicone mold and left to cure for 28 days. It can be placed at a hardening or fluid state by simply adjusting the amount of water. After hardening, the natural rocks mortar replicas are removed

from the molds, and will then be used as rock sidewall. After 28 days of curing, the average unconfined compressive strength (UCS) was around 56 MPa. Four granite surfaces (G1 to G4) and four schist surfaces (S1 to S4) were molded for artificial rocks mortar replicas. The surface of the specimens was characterized using the specific surface roughness coefficient SRs (Belem et al., 2000). SRs varies from 5.1% to 7.0% for granite surfaces, and from 11.1% to 18.5% for schist surfaces. Schist surfaces are then rougher than the granite surfaces. It should be mentioned that the amplitude of the schist surface topography is greater than that of the granite surface and that the schistosity is somehow directional. Granite surface exhibits isotropic morphology.

EXPERIMENTAL PROGRAM

Paste backfill–rock mortar replica specimens preparation

For the cemented paste backfill preparation, the required masses of tailings, water and binder (20% of type GU Portland cement and 80% of GBFS) were mixed and kneaded using a Hobart mixer for about 10 minutes. The slump height was about 180±2 mm, which corresponds to a solid mass concentration Cw% of 76% (= 100*(100/[100+w%]); where w% is the water content). The fresh CPB is then poured over the surface of artificial rock mortar replica using 120×120×65 mm PVC molds in order to create the interface between CPB and rock wall. After casting, the CPB samples were cured in a humid chamber at 23 ± 2° C and > 90% R.H. The final dimensions of each assembled specimen (CPB–rock wall mortar replica) after demoulding were 116×116×120 mm. The average unconfined compressive strength (UCS) values of the CPB triplicate specimens were 522 kPa at 14 days of curing and 1 212 kPa at 28 days.

Shear test on backfill–artificial rock mortar replica interfaces

The direct shear tests were performed on cemented paste backfill–artificial rock wall interfaces in order to assess the frictional shear strength parameters and shear bond strengths. The direct shear apparatus generates pressure using a hydraulic pump. This pressure allows the sample to shear through the relative displacement of two half-shear boxes (one fixed and one movable). The fixed lower half-box contains the artificial rock specimen, and the upper movable half-box contains the CPB specimen.

Testing was performed on the granite rock interfaces (G1 and G3) and the schist rock interfaces (S1 and S4). For each curing time and for each interface, three CPB–rock surface specimens were used for three different applied normal stresses (50, 100 and 150 kPa). A constant shear rate of 1 mm/min and a total shear displacement of 10 mm were used. The shear stress–shear displacement curves were used for determining the failure envelope and its corresponding criterion. Only one 14-day specimen was used at a low normal stress (5 kPa) for the determination of the interfacial shear bond strength. The CPB–mortar rock interfaces were G1, G2 and G3 for the granite surface, and S1, S2 and S3 for the schist surface. A very low constant shear rate of 0.05 mm/min and a total shear displacement of 8 mm were used.

RESULTS AND DISCUSSION

The shear test results can be represented by graphs of shear stress - shear displacement u curves, normal displacement v-shear displacement u curves and peak shear stress τ_p-normal stress σ_n curves. The τ_p - σ_n curves are used for determining the failure envelope according to the Mohr–Coulomb criterion:

$$\tau_p = c_x + \sigma_n \tan\varphi_j \qquad (1)$$

where:

c=cohesion;

x=a (c_a) for apparent or adhesion;

x=b (c_b) for bond;

φ_j=interface friction angle.

The value of the peak shear stress τ_p at $\sigma_n = 0$ corresponds to: (i) the apparent cohesion or adhesion ($c_x = c_a$) of a non-bonded joint or interface, and (ii) the bonding cohesion ($c_x = c_b$) of a bonded joint.

Shear stress–shear displacement curves

For each type of rock mortar replica, only the results from one surface are presented, namely G1 for the granite surface and S1 for the schist surface (Fig. 1 and 2). The shear stress-shear displacement curves can be divided into four stages. Stage 1 corresponds to an initial peak shear stress associated with the shear bond strength. At this stage, the shear stress increases with the shear displacement until it reaches an initial peak at a shear displacement ranging between 2 and 3 mm. According to Kodikara and Johnston (1994), this stage could correspond to the breakage of the cement bonding. At stage 2, a slight decrease is observed in the shear stress as the shear displacement increases. It happens after the breakage of the surface bonding that produces a slip on the interface of both surfaces. Stage 3 is characterized by an increase in the shear stress as the shear displacement increases until it reaches the interface peak shear stress (friction). This happens because the interface asperities contact area or the contact at the CPB-rock interface decreases with displacement, causing the increase of the contact load and stress until the local stress on the CPB major asperity (critical stress) exceeds its shear strength. Because the CPB major asperities cannot carry the load at this critical stress, it fails. However, some strong CPB asperities may not have been damaged during this stage. At stage 4, the surface of the CPB has most suffered damage because of its low strength compared to the mortar rock (schist or granite). After the crushing of CPB asperities, slippage occurs reducing the shear stress. After stage 4, some stick-slip behavior can be observed, but is mostly characterized by a relatively constant shear stress, or a slight decrease in shear stress, as the shear displacement increases. This can result from both sliding – overriding at the interface and damage of some weaker asperities during shearing (Indraratna and Jayanathan, 2005). It can be due to: (i) the contribution of some strong undamaged asperities to shear stress, and (ii) the CPB particles (tailings) slide or roll over the mortar rock, and the presence of friction between tailings particles themselves and the mortar rock surface.

Indeed, the observation of the mortar rock interface after testing confirms this assumption, because much of the CPB's asperities have broken. For the normal displacement-shear displacement curves, three stages can be observed (i.e. Fig. 1a)). The first part is a significant contraction corresponding to the normal stress application. This initial normal displacement corresponds to the maximum compressibility that the CPB can withstand under the applied normal stress.

The initial normal displacement increases with the normal stress ($\sigma_n = 150$ kPa). The second part of the normal displacement-shear displacement curves shows a relatively constant normal displacement in the ranges 0–3 mm and it corresponds to stages 1 and 2 of the shear stress-shear displacement curves, characterized by a cement bond between CPB and the mortar. No normal displacement was observed during this stage. The last part is characterized by dilation: rolling and sliding of CPB particles over the mortar rock surface increase normal displacement.

Shear strength parameters

Table 1 summarizes the cohesive strength and the interfacial angle of friction for granite G1 and G3 and for schist S1 and S4. The variation of the shear strength depends mostly on the mortar rock surface roughness.

The bonding cohesion c_b varies in the range 65-115 kPa, while the interfacial angle of friction φ_j varies in the ranges 45-52°. These results show that for a given interface, the CPB curing time does not have a great impact on the values of the interfacial shear parameters, contrary to surface roughness. Koupouli *et al.* (2015) showed that for a CPB matrix, having the same characteristics as those presented here, the internal cohesion c' varies from 130–340 kPa, while the internal friction angle φ' varies from 39–43°. Therefore, according to the results of this study, $c' > c_b$ and $\varphi' < \varphi_j$.

Interfacial shear bond test results

Figure 3 presents the shear stress–shear displacement curves for the granite (Fig. 3(a)) and schist (Fig. 3(b)) interfaces. In general, two stages can be observed. A first elastic plastic loading with a plateau (stage 2) followed by a stress increase until a peak was reached (stage 1) before the stress drop (stress softening stage). The peak shear stress corresponds to the interface shear bond strength (or adhesive strength). Two strength parameters can be obtained, namely the cement bond strength (τ_p, stage 1) and the peak shear stress (τ_p, stage 2) observed at the mortar rock and CPB interface during frictional sliding after cement bond breakage. Taking into account the uncertainties of the measures, the shear bond strength τ_b is approximately 10 kPa for the granite interface G1, 11 kPa for granite G2, and 17 kPa for the granite G3 mortar replicas. For the interface of schist S1, S2 and S3 mortar replicas, τ_b is approximately 10 kPa. The shear bond strength is reached when the displacement is between 1 and 2 mm.
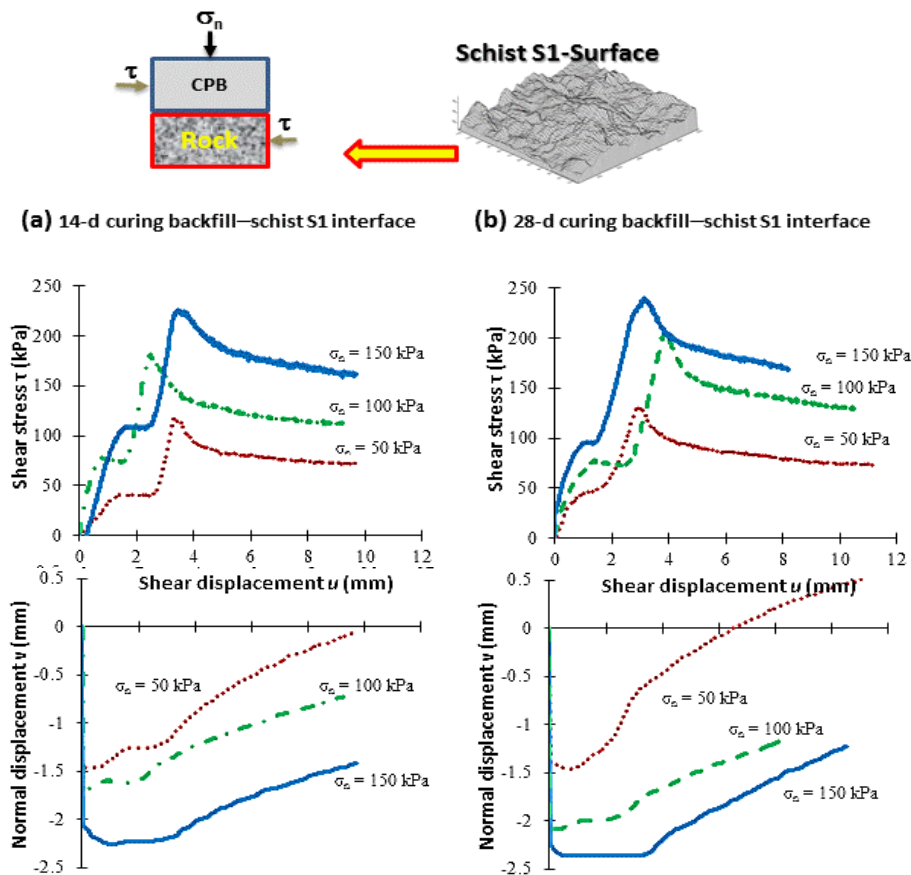

Fig. 1. Shear stress−shear displacement−normal displacement curves for S1: (a) 14 days curing (b) 28 days curing.
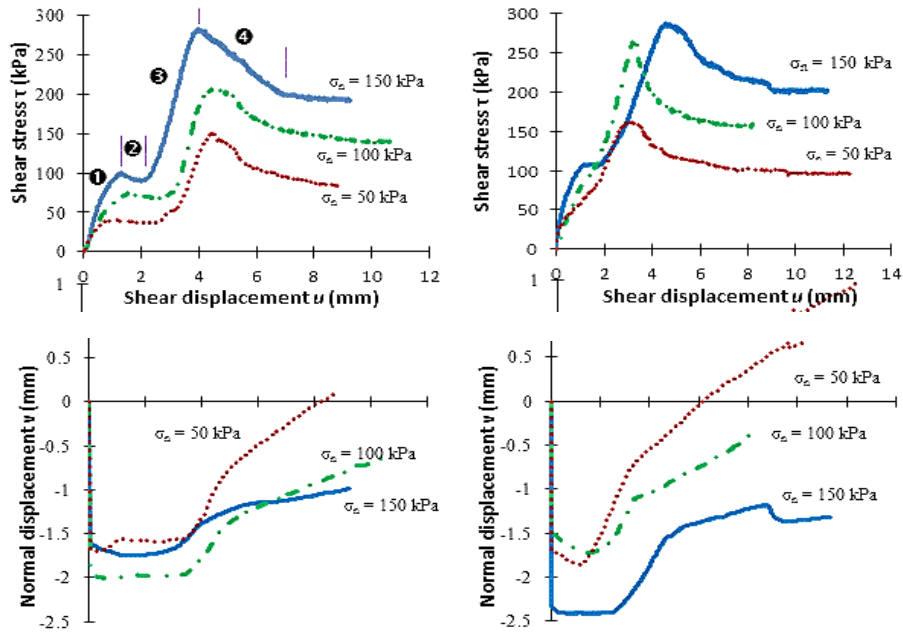
Fig. 2. Shear stress–shear displacement–normal displacement curves for G1: (a) 14 days curing (b) 28 days curing.

Table 1. Shear strength parameters of granite (G1 and G3) and schist (S1 and S4) surface mortar replicas.

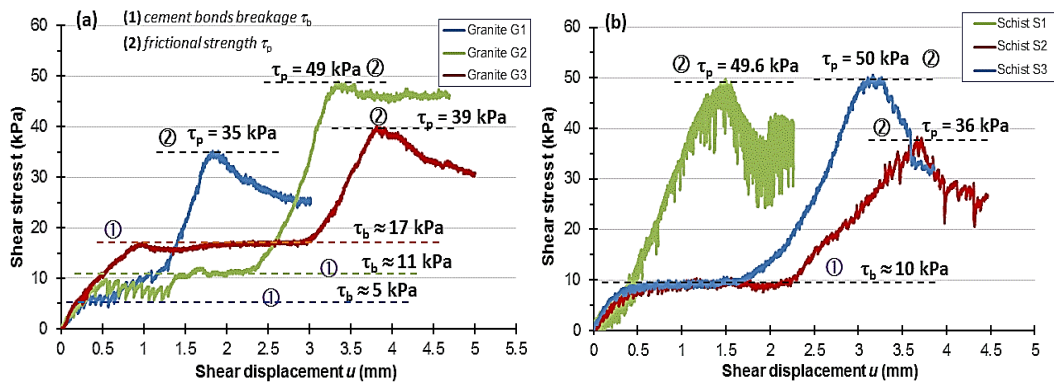|	Interface bonding cohesion c_b (kPa)		Interface angle of friction φ_j (°)	
	14-day curing	28-day curing	14-day curing	28-day curing
Granite G1	68	78	46	49
Granite G3	65	68	51	45
Schist S1	90	115	51	52
Schist S4	82	70	46	51

Fig. 3. Interfacial shear bond curves at the CPB–mortar rock interface: (a) granite G1, G2 and G3; and, (b) schist S1, S2 and S3 (14-day curing time).

CONCLUSION

This paper investigated the impact of paste fill (CPB) curing time and roughness of mortar replicas of natural rock surfaces (schist and granite) on the shear strength parameters of CPB–mortar replica interfaces. In general, it appears that the CPB curing time has no impact on the shear strength, but the roughness at the interface does. The following conclusions can be drawn:

• The shear strength τ_p of the granite surface mortar replicas (G1 and G3) varies from 120–245 kPa.

• For the schist interfaces (S1 and S4), which are rougher than the granite interfaces, τ_p varies from 130–293 kPa.

• The cement bond cohesion c_b varies in the ranges 65-115 kPa (lower than the internal cohesion c' of the CPB matrix).

• The interfacial friction angle φ_j varies in the ranges 45-52° (higher than the internal friction angle φ' of the CPB matrix).

• The shear bond strength τ_b varies between 10 and 17 kPa for granite and schist surface mortar replicas.

The results of these tests will allow estimating the short-term shear strength that develops at the backfill–rock sidewall interface, which is believed to be responsible for the arching effects occurrence in backfilled stopes. The results will also be useful for better theoretical estimates of the pressure distribution in a backfilled stope using analytical solutions that take the arching effect into account.

REFERENCES

Belem, T., & Benzaazoua, M. (2008). Design and application of underground mine paste backfill technology. In *Geotechnical and Geological Engineering* (Vol. 26, Issue 2). https://doi.org/10.1007/s10706-007-9154-3

Belem, T., Benzaazoua, M., & Bussière, B. (2000). Mechanical behaviour of cemented paste backfill. *Proceedings of 53rd Candadian Geotechnical Conference*, *1*(February 2016).

Belem, T., Benzaazoua, M., El-Aatar, O., & Yilmaz, E. (2013). Effect of drainage and the pore water pressure dissipation on the backfilling sequencing. *23rd Word Mining Congress*.

Belem, T., Homand-Etienne, F., & Souley, M. (2000). Quantitative parameters for rock joint surface roughness. *Rock Mechanics and Rock Engineering*, *33*(4). https://doi.org/10.1007/s006030070001

De Souza, E., Archibald, J., & Beauchamp, L. (2009). Compilation of industry practices for control of hazards associated with backfill in underground mines-Part I surface and plant operations. In *Proceedings of the 3rd Canada-US (CANUS) Rock Mechanics Symposium (RockEng09). Toronto, Canada: Canadian Rock Mechanics Association* (p. 12).

Fall, M., & Nasir, O. (2010). Mechanical Behaviour of the Interface Between Cemented Tailings Backfill and Retaining Structures Under Shear Loads. *Geotechnical and Geological Engineering*, *28*(6). https://doi.org/10.1007/s10706-010-9338-0

Fourie, A., Helinski, M., & Fahey, M. (2007). Using effective stress theory to characterize the behaviour of backfill. *CIM MAGAZINE*, *100*(1103), N-A.

Indraratna, B., & Jayanathan, M. (2005). Measurement of pore water pressure of clay-infilled rock joints during triaxial shearing. *Geotechnique*, *55*(10), 759-764.

Kodikara, J. K., & Johnston, I. W. (1994). Shear behaviour of irregular triangular rock-concrete joints. *International Journal of Rock Mechanics and Mining Sciences And*, *31*(4). https://doi.org/10.1016/0148-9062(94)90900-8

Koupouli, N. J. F., Belem, T., Rivard, P., & Effenguet, H. (2016). Direct shear tests on cemented paste backfill–rock wall and cemented paste backfill–backfill interfaces. *Journal*

of Rock Mechanics and Geotechnical Engineering, *8*(4). https://doi.org/10.1016/j.jrmge.2016.02.001

Landriault, D. A. (1995). The present state of paste fill in Canadian underground mining. In *97^< th> Annual General Meeting of CIM Rock Mechanics and Strata Control* (pp. 229-238).

le Roux, K., Bawden, W. F., & Grabinsky, M. F. (2005). Field properties of cemented paste backfill at the Golden Giant mine. *Institution of Mining and Metallurgy. Transactions. Section A: Mining Technology*, *114*(2). https://doi.org/10.1179/037178405X44557

Manaras, S. (2009). *Investigations of backfill-rock mass interface failure mechanisms*. Queen's University (Canada).

Mitchell, R. J., Olsen, R. S., & Smith, J. D. (1982). Model studies on cemented tailings used in mine backfill. *Canadian Geotechnical Journal*, *19*(1). https://doi.org/10.1139/t82-002

Mitchell, R. J. (1989). Stability of cemented tailings backfill. *Computer and physical modelling in geotechnical engineering. Balkema, Rotterdam*, 501-507.

Mitchell, R. J. (1989). Model studies on the stability of confined fills. *Canadian Geotechnical Journal*, *26*(2). https://doi.org/10.1139/t89-030

Nasir, O., & Fall, M. (2008). Shear behaviour of cemented pastefill-rock interfaces. *Engineering Geology*, *101*(3–4). https://doi.org/10.1016/j.enggeo.2008.04.010

Potvin, Y., Thomas, E., & Fourie, A. (2005). Handbook on mine fill. In *Not available* (p. 179). Australian Centre for Geomechanics.